Spring 2020

Assessing Morphology of ipRGCs After Traumatic Brain Injury

Brian Foresi
The University of Akron, bf39@zips.uakron.edu

Matt Smith
Northeast Ohio Medical University, msmith13@neomed.edu

vAssessing the vulnerability of intrinsically photoreceptive ganglion cells (ipRGCs) in a murine model of mild traumatic brain injury (mTBI)

A Thesis

Presented in partial fulfillment of the requirements for the Honors Research Project in the Williams Honor College of The University of Akron

Brian D. Foresi

Department of Biology

2020

Thesis Committee:
Dr. Matthew A. Smith, Ph.D. (Project Sponsor)
Dr. Jordan M. Renna, PhD (Reader)
Mr. Thibaut Houette (Reader)

Abstract

Vision-related symptoms are one of the most common effects experienced after a concussion/mild traumatic brain injury regardless of age. Heightened sensitivity to light, and disturbances in sleep patterns are two of the most frequently diagnosed. While the exact etiology of these symptoms remains unknown, evidence suggest the potential involvement of intrinsically photosensitive ganglion cells (ipRGCs) which uniquely innervate both retinal and brain targets involved in photic adaptation and circadian rhythm regulation. Variation in ipRGC structure and function have been reported in other neurodegeneration conditions such as Parkinson's, Alzheimer's, glaucoma, and diabetic retinotopy, however, a direct assessment of ipRGCs after brain trauma remains incomplete. The current study investigated retinal ipRGCs morphometrics and anatomical integrity of injury induced neuroinflammation patters in ipRGC brain projection sites in a murine model of mild traumatic brain injury. The resulting data show significant dendritic and somal modifications in the retina, with ipRGCs of injured subjects with accompaniment of neuroinflammation in corresponding brain projections sites. These findings though preliminary illuminate the vulnerability of these unique retinal neurons to brain trauma and support additional investigation to fully characterize their role in the post-concussion visual syndrome paradigm.

1. Introduction

1.1. Definitions and Epidemiology

Traumatic brain injury (TBI) is defined as a disruption in normal functions of the brain caused by a bump, blow, jolt to the head, or penetrating head injury (CDC, 2014). More specifically, TBI encompasses the functional deficits, neuroinflammation, and abnormal brain metabolism that is maintained for days to months after one of these traumatic events (Nilsson et al., 2019). Often times TBI is confused with concussion despite the differences in their symptomologies. Concussion, unlike TBI, presents abrupt symptoms resulting from a traumatic event to the brain and has a spontaneous recovery (Nilsson et al., 2019). Sometimes concussions are synonymously noted as mild traumatic brain injury (mTBI) which is a somewhat inappropriate nomenclature considering TBI's distinctly separate characterization. Loss of consciousness and other transient symptoms are therefore concussion related and not an aspect of the TBI process. The spontaneity of recovery of concussions prevents it from being a treatable condition, rather a warning for resulting TBI. The TBI pathological cascade of events can cause disastrous neurological impairment and if activated enough leads to neurological disease. This disease has been characterized as chronic traumatic encephalopathy (CTE) and is associated with progressive neurodegeneration and significant, lasting cognitive deficits (Nilsson et al., 2019). Being that TBI is a result of concussion and a link to more debilitating CTE, the clinical relevance in this neurological impairment is profound especially when realizing TBI is not able to be treated directly.

High incidence of mTBI provides additional clinical relevance for the study of this disease process. The highest rates of TBI are in children and young adults at a rate of 1081 per 100,000 and 1591 per 100,000 people respectively. This age group commonly occur these injuries during sports and are incentivized to lower their recovery time as evident by extensive return to play guidelines to enforce proper recovery times (Coxe et al., 2018). It is important to note that the age cohort of adults ≥75 years represent another high TBI affected population with 2232 cases per 100,000 people but has less cases than all people under 18 years old.

One of the main challenged in the search for TBI treatment is the classification of disease severity. Like many disease processes, TBI has a variation of pathologies that cannot all be treated in the same way and will require accurate classification to be effective (Sidney Kimmel Medical College). Classification of traumatic brain injury severity has previously been identified

with a variety of methods including the Glasgow Coma Scale (GCS), Abbreviated Injury Scale (AIS), and various versions of the Sports Concussion Assessment Tool (SCAT) (Rodgers, 2018, Sargeant et al., 2018). Research is constantly being performed for a more specific classification system to more accurately group pathophysiological mechanisms (Saatman et al., 2010). The categories laid out in many of these methods however still lead to improper classification and diagnostics to properly triage TBI patients (Lu et al., 2012). More mild TBI patients potentially assume the most risk in this situation as they are often misdiagnosed and are left out of treatment attempts. As a result, they often develop symptoms months later (Jones and Jarvis, 2017).

1.2 Role of Neuroinflammation and the Secondary Cascade

One of the reasons for poor diagnostic development is due to the wide spanning effects of TBI. A look into the molecular basis of TBI can illustrate why diagnostics and treatment options remain ineffective. Beginning with the primary injury at the point of bump, blow, jolt, or penetration, along with the immediate effects, stimulates a cascade of varying pathologies. These include disruptions to cerebral blood flow causing edemas, increases in intracellular calcium of neurons, and the activation of catabolic proteins leading to neuronal degradation (Dickson and Weller, 2011). This diffuse neuronal trauma, similar to the peripheral responses to injury, is exacerbated with the release of proinflammatory cytokines by glial cells that bathe surrounding tissue. This results in a widespread secondary neurodegenerative cascade which has many different aspects, two of which being astrocytes and microgliosis (Dickson and Weller, 2011). Astrocytosis is characterized by hypertrophy and proliferation of reactive astrocytes in areas of injury within the brain (Sofroniew and Vinters, 2010). An important characteristic of astrocytosis is the upregulation of glial fibrillary acid protein (GFAP) at all levels of pathological severity. GFAP is a protein that is expressed by reactive astrocytes which are only seen under normal conditions in a subset of white matter tracts (Sofroniew and Vinters, 2010). Therefore, GFAP is a relevant biomarker that can be used to assess the presence of neuroinflammation and the integrity of brain tissue post-injury. Another aspect of the secondary neurodegenerative inflammatory response is the proliferation of activated microglia. Activated microglial while are beneficial in helping clean up and remove damaged neurons (Kettenmann et al., 2011) can become detrimental with sustained activity leading to stripping and phagocytosis of non-damaged, normal functioning synapse in adjacent and distal after injury, thus perpetuating the neurodegenerative cascade (Hammond et al., 2018). Adding to the diffuse character of TBI

pathology is microglial migration in amoebic form with evidence of migration as early as 24 hours post-injury (Morgese et al., 1983). Microglia are able to be identified *in vivo* by the protein, ionized calcium binding adaptor molecule (IBA1) (Kettenmann et al., 2011). Additionally, it has been identified that IBA1 concentrations increase after the activation of microglia indicating a positive correlation between microgliosis and expression levels (Kettenmann et al., 2011).

Discussing the relationship of cytokines, astrocytes, and microglia can highlight the molecular aspects of TBI relevant in this study. The initial injury prompts local astrocytes and microglia to release proinflammatory cytokines while simultaneously adjusting their gene expression profiles (Jeon & Kim, 2016). These responses cause astrocytosis and microgliosis of the local glia and the proinflammatory cytokines spread out randomly in the brain to activate more glial cells, perpetuating a cycle of gliosis (Dickson & Weller, 2011). This can be visualized in the brain post-mortem with the GFAP and IBA1 biomarkers which are upregulated as a part of the gene profile expression change.

1.3 Role of the Visual System in TBI

Visual related symptoms are common due to the large percentage of the brain dedicated to visual pathway integration. The diffuse nature of TBIs therefore has a high chance of influencing pathways for these functions (Keller, 2012). Additionally, there are a host of symptoms with high prevalence in TBI patients related to non-image forming pathways such as photosensitivity or photophobia and circadian rhythm disruptions which are normally indicated by sleep disruptions (Barshikar and Bell, 2017).

The retina contains many different types of cells including ganglion cells which are neurons sending visual information to the brain. There are many types of ganglion cells including a specialized set which are able to convert light directly into electrical potentials and are therefore called intrinsically photoreceptive retinal ganglion cells (ipRCGs). Because of these cells' unique projection percentage to regions of the brain with significant functional overlap with TBI symptoms, they may be important in the case of TBI (Cui et al., 2015, Hattar et al., 2010). In general, this relationship has not been given much attention in the literature. One study assessing ipRGC function after TBI in military veterans showed an increase in photo potentiation response from TBI patients compared to controls (Hartwick, 2015). This is indicative of ipRGCs being less able to adapt to light after a TBI which would represent an

obvious dysfunction from normal physiological function. The study however did not investigate ipRGC morphological changes between patients, only the difference in functional response. This leaves room for the exploration of morphological studies to more accurately investigate how ipRGCs might be influenced after a TBI.

This project will attempt to identify a relationship between TBI and consequent ipRGC morphology. This relationship is important because there may be clinical relevance of diagnostics and interventional methods for TBI if the ipRGC dysfunctional context is better understood. A benefit of an ipRGC linkage is that it could associate TBI with changes in the eye, which is much more accessible to practitioners than the brain. Additionally, visually related symptomologies, like photophobia and circadian rhythm disruption, have significant bodies of research which can potentially be linked together with an ipRGC and TBI relationship (Hayne and Martin, 2019, Aoun et al., 2019). To assess this potential impact on ipRGCS, this study will identify if a morphological change in ipRGCs will result after TBI in a mouse model. The reason for injuring the visual cortex is to identify if the pathological response from more distal neurons to the ipRGCs will cause their preferential morphological change (Hubel and Wiesel, 1972). Though a TBI can disrupt deeper brain anatomy, it will likely have more of an impact on the more superficial structures, especially more moderate TBIs. Having the CCI in the cortex rather than performing a lesion study more closely models the TBI injury paradigm (Osier and Dixon, 2018).

2. Methods

2.1 Subjects

Male and female C57BL/6 mice were used in this study (Jackson Labs, stock # 000664). This strain is one of the most widely used strains in biomedical research and do not develop any retino-ocualar phenotypes making them best suited for this study. All mice were maintained in a 12-hour light/dark cycle with water and standard rodent chow available ad libitum and housed in the same room under the same environmental conditions in the Comparative Medicine Unit at the Northeast Ohio Medical University (NEOMED). All experimental procedures were approved by the NEOMED Institutional Animal Care and Use Committee and conducted in accordance

with the Guide for Care and Use of Laboratory Animals published by the National Institutes of Health.

2.2 Groups, Sample Size, and Ages

Sixteen subjects were equally assigned into two-procedural groups: 1) Injury and 2) Control (Sham). Each procedural group utilized subjects in two-age groups: 1-month and 5-months. Age ranges were based on human equivalents to reflect an immature pediatric (1-month old mouse ≈ 12.5-year old human) and mature young adult (5-month old mouse ≈ 27-year old human) population (Flurkey et al., 2007).

2.3 Controlled Cortical Impact Injury Model

Controlled cortical impact (CCI) is a well-established and widely used model of brain trauma that uses an electromagnetically controlled piston to induce a controlled, reproducible injury to an anesthetized animal subject secured within a stereotaxic apparatus (Osier and Dixon, 2018).

Mice were anesthetized with 3% inhaled isoflurane anesthesia and placed prone into a stereotaxic apparatus (Stoelting, Wood Dale, IL) with a nose cone delivering 2.5% isoflurane at 0.8 ml/min. Normal body temperature was maintained using thermal heating elements underneath stereotaxic base. Scalp was shaved and sterilized with isopropyl alcohol and betadine solutions. To prevent eye drying and irritation topical GenTeal Tears gel (0.3 % Hypromellose) was applied. A midsagittal incision was performed to expose skull sutures. A craniotomy leaving dura intact was performed using 2-mm trephine over primary visual cortex (4.8 mm posterior and 2.5 mm from bregma). Following the craniotomy, the CCI impactor (1.5-mm diameter) was positioned within the cranial window to deliver single non-repeating impact (speed of 2 meters/second, dwell time of 100 millisecond at a depth of 0.4 mm) to induce a mild traumatic brain injury within primary visual cortex. Following impact, the craniotomy was sealed using bone wax and the scalp was closed using VetBond tissue adhesive (3M).

Additionally, mice received 1µl intravitreal injections of cholera toxin subunit-B conjugated to CF-488 (CTB488; Biotium) using 33-ga. Hamilton Syringe. CTB is readily taken

up and transported down the axons of RGCs and is used to safety and effectively locate retinal projections sites in post-mortem brain tissue.

Following completion of surgical procedures, mice were allowed to fully recover from sedation and observed for any non-expected signs of stress or dysfunction before being returned to CMU. Observation of gross motor, pain, balance dysfunction, would indicate a more diffuse injury context than intended constituting removal from the study. Subjects within the control groups underwent a sham surgical procedure which replicated all aforementioned including craniotomy but did not receive a controlled cortical impact.

2.4 Tissue Collection

All subjects one-week following surgery were sacrificed via anesthetic overdose (Fatal Plus, 120 mg/kg, i.p.) and were then transcardially perfused with 4% paraformaldehyde (PFA)/0.1M phosphate buffered saline (PBS). Whole eyes and brains were dissected from the skull, post-fixed for 1-hour and overnight in 4% buffered PFA, respectively. Retinas were dissected from the eyes, vitreous removed, and maintained as whole mount preparations for immunofluorescent staining. Brains were cryoprotected in 20% sucrose/PBS prior to sectioning. Coronal sections were taken at 40µm on a freezing/sliding microtome.

2.5 Immunofluorescence (IF)

Whole-mount retina along with alternate series of brain sections containing the lateral geniculate nucleus (LGN), olivary pretectal nucleus (OPN), and suprachiasmatic nucleus (SCN) were assayed using IF labeling methods. Tissue was incubated at 37° C for 1 hour in a blocking solution containing 5% normal donkey serum and 0.1% Triton-X 100 in PBS, followed by overnight incubation at room temperature in a primary antibody solution containing 3% serum, 0.1% Triton. Primary antibodies were used to label intrinsically photoreceptive ganglion cells in the retina (Anti-Melanopsin, 1:500; AB-N39, Advanced Targeting Systems), parenchymal reactive astrocytes (Anti-Glial fibrillary acidic protic, GFAP; 1:500; Millipore MAB360), and microglia/macrophages (Anti-ionized calcium-binding adapter molecule 1, IBA1; 1:500; Abcam ab5076). After primary incubation, tissue was washed 3x in PBS for 10 minutes and then

incubated at room temperature for 2 hours in CF-Dye conjugated (594, 647, and 755 dyes) secondary antibody solution (Biotium, San Francisco, CA) at a dilution of 1:200 in PBS containing 1% serum and 0.1% Triton. After 3 final PBS washes (10 minutes each), tissue was mounted onto slides and coverslipped ProLong Glass with NucBlue (ThermoFisher).

2.6 Microscopy

Retina and brain tissue samples were imaged on a Zeiss Axio Imager M2 (Hamamatsu Flash4.0 V3 Digital CMOS; Japan) epifluorescent microscope equipped with an Apotome.2 structured illumination system for obtaining optically sectioned images, a motorized Z and X-Y stage, and Zen 2 operating software with deconvolution, tiling, and extended-depth-of-focus modules. Retinal whole-mount reconstructions were obtained by imaging for Melanopsin immunofluorescence using the Plan-Apochromat 20x/0.8 objective across multiple adjacent frames with 10% overlap. Multi-frame tiles were stitched using the Zen Pro 2.3 software (Zeiss; Jena, Germany) to eliminate overlap. To assess parenchymal inflammation across ipRGCs projections sites, we used intravitreal transported CTB-488 florescent signal to help locate projection sites and then captured IBA1 and GFAP label with region of interest using Axio Imager/apotome system.

2.7 Data Analysis

Image Pro Premier software (Media Cybernetics) was used to generate automated counts of Melanopsin labelled RGCs soma from images of whole-mount retina (adapted from Dengler-Crish et al., 2014) as well as determine somal size and number of dendritic branch points. For Melanopsin -positive RGC in each retina were plotted and then the total was then divided by the total area (mm2) of the retina to compute ipRGC density. For somal and dendritic analysis a sub-sampling of 5-10 melanopsin-positive RGCs restricted to the dorsal retina were analyzed axons all groups.

2.8 Statistical Analysis

All statistical analyses were conducted using SPSS software (IBM; Armonk, NY). A 2 x 2 factorial analyses of variance (ANOVA) were used to test for main effects of injury condition (Injured; Non-injured) and age (1-month, 5-month) as well as for significant interactions for each dependent variable of interest (cell density, somal area, number of branch points). Bonferroni-corrected post-hoc tests were used to assess subgroup differences.

3. Results

3.1 ipRGCs morphological is altered in post-TBI retina

Melanopsin stained ipRGCs in the contralateral dorsal retina of 1-month old mice following mTBI revealed a significant reduction in number of dendritic branching ($F_{3,16} = 10.63$, $p < 0.05$; Figure 1A&B) and somal area ($F_{3,16} = 8.76$, $p < 0.05$; Figure 1C) compared to age-matched non-injured controls. Unlike the 1-month old subjects, injured 5-month old subjects did not show a statically significant difference in ipRGC dendric arbor complexity ($F_{3,16} = 8.76$, $p < 0.05$; Figure 1B), however, 5-month old injured ipRGC soma were significantly smaller compared to non-injured controls ($F_{3,16} = 8.76$, $p < 0.05$; Figure 1B) and to ipRGC soma in injured 1-month old retina ($F_{3,16} = 8.76$, $p < 0.05$; Figure 1B).

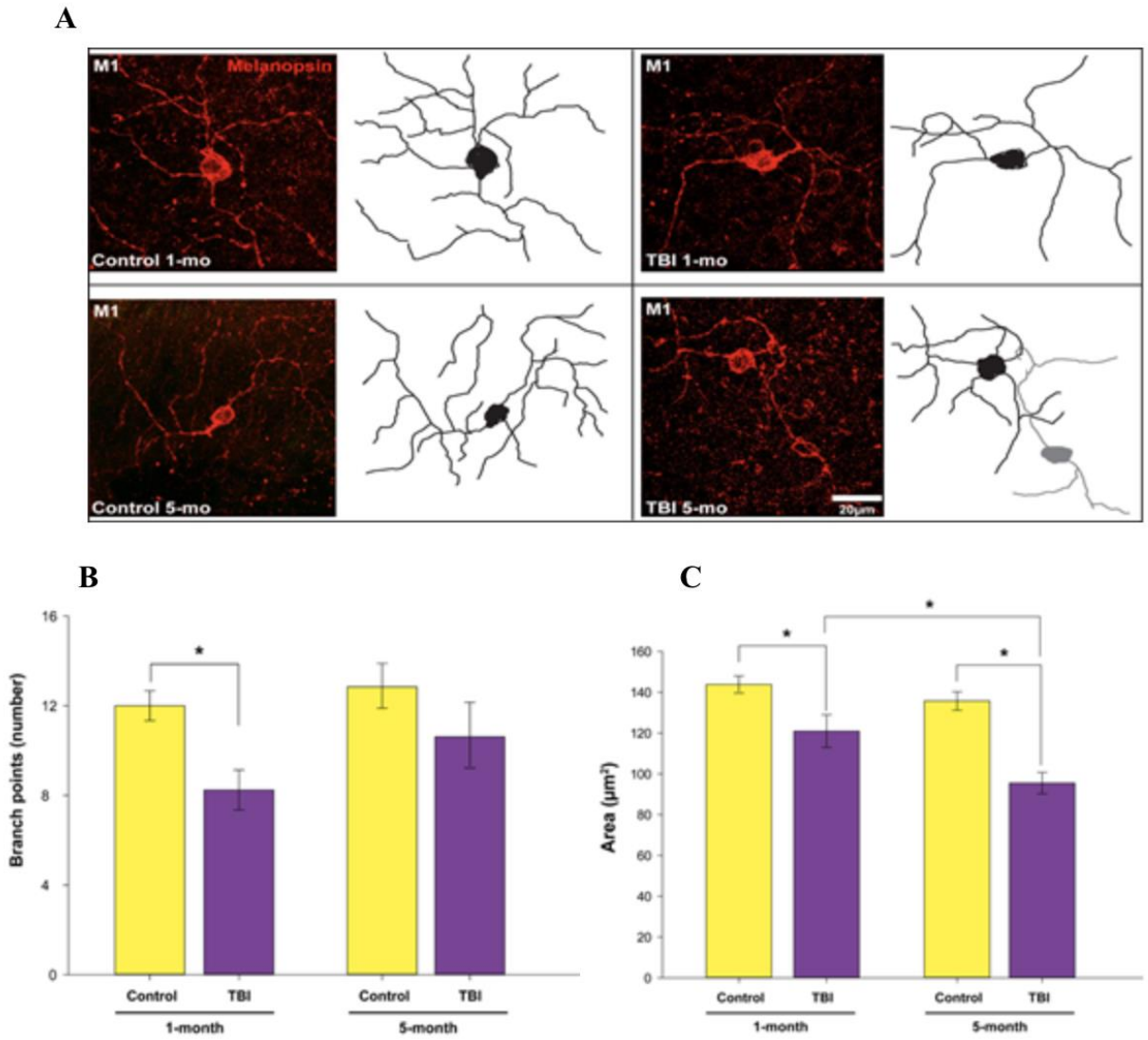

Figure 1. Flat mounted melanopsin stained ipRGC (red) images and tracing from a; 1 month old (top row) 5-month (bottom row) old control (left) and TBI (right) mouse retina. From this image it can be seen that ipRGCs in TBI retina exhibit less complex arborization pattern than compared to non-injured age-matched controls. (BAR GRAPH) Number of branch points plotted across experimental and control groups. 1- month old mouse retina graphed on the left with control and TBI retina being represented by yellow and purple bars respectively. 5-month-old mouse retina graphed on the right with control and TBI retina also being represented by yellow and purple bars respectively. Each bar height represents that average branch point count of the analyzed ipRGCs along with standard error bars. Somal area in μm^2 is plotted across experimental and control groups. 1 month old mouse retina graphed on the left with control and TBI retina being represented by yellow and purple bars respectively. 5 month old mouse retina graphed on the right with control and TBI retina also being represented by yellow and purple bars respectively. Each bar height represents that somal area of the analyzed ipRGCs along with standard error bars. The star represents significant differences of $p<0.05$.

3.2 Age-dependent loss of IpRGCs post TBI

Cell density is another morphological metric. This measurement indicates an extreme morphological pattern of apoptosis where the entire morphology of the cell degrades. The extent of apoptosis can be indicated by cell density whereas the lower cell density can indicate a higher incidence of apoptosis. In Figure 4 the cell densities across the four groups can be seen to see which have been influenced by this extreme morphological change. The graph illustrates that the 5 month TBI retinas had a lower cell density compared to the controls. Additionally, it can be seen that both the one month groups and the 5 month control were found to have no statistical difference in cell density. These results are evident of a preferential effect in older mice as the only statistical difference was between the 5 month groups.

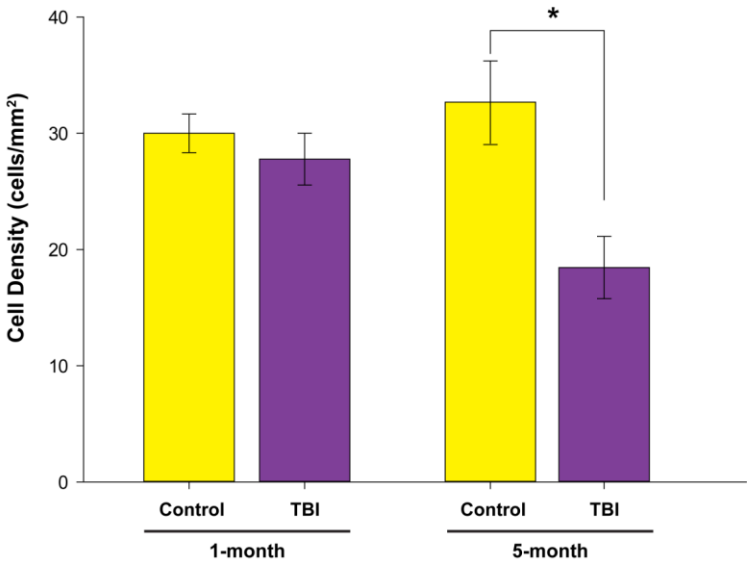

Figure 2. Cell density as cells/mm^2 is plotted across experimental and control groups. 1 month old mouse retina graphed on the left with control and TBI retina being represented by yellow and purple bars respectively. 5 month old mouse retina graphed on the right with control and TBI retina also being represented by yellow and purple bars respectively. Each bar height represents that somal density of the [redacted]analyzed ipRGCs along with standard error bars. The star represents significant differences of $p<0.05$.

3.3.Neuroinflammation in ipRGC brain projection sites

CTB488 staining, in green, identified structures in the brain directly synapsing with ipRGCs. This allowed for the outlining of the suprachiasmatic nucleus (SCN) in Figure 3, the olivary pretectal nucleus (OPN) in Figure 4, and the lateral geniculate nucleus (LGN) in Figure

5. The SCN of 1 month mTBI mice exhibited higher GFAP and IBA1 labeling qualitatively compared to age-matched non-injured controls (Figure 3 columns 3&4). The OPN did not show qualitative differences in labeling between 1 and 5 month mTBI mice compared to the 1 month non-injured control (Figure 4 columns 3&4). Finally, the LGN showed a unique pattern of GFAP and IBA labeling. The 1 month mTBI and age matched controls showed no qualitative difference in LGN labeling (Figure 5 columns 3&4, rows 1&2). The 5 month mTBI LGN however did show an increase in labeling compared to both one month mice, but only in the inter geniculate leaflet (IGL) (Figure 5 columns 3&4).

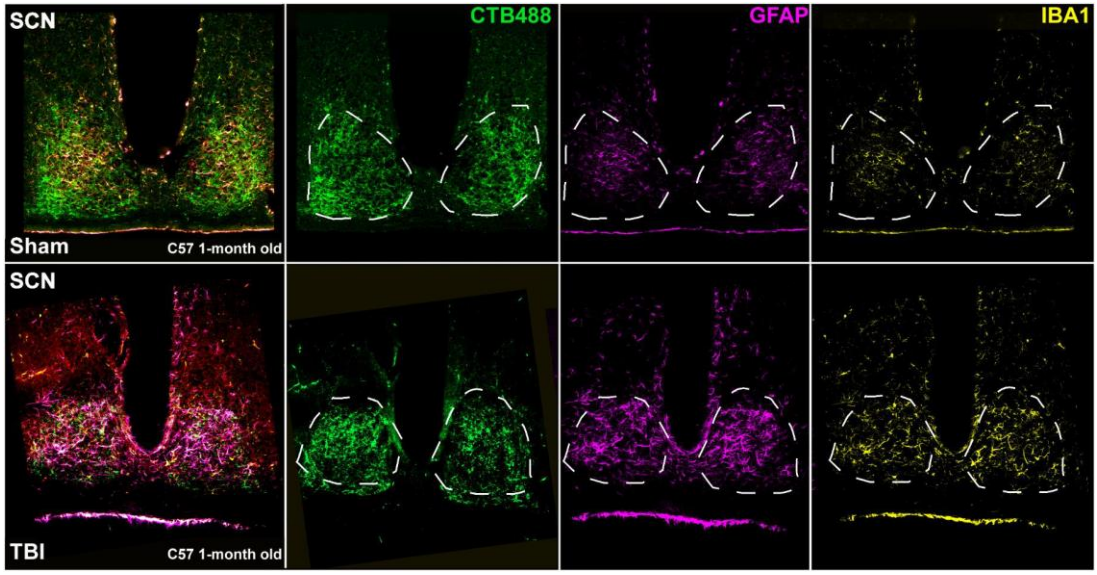

Figure 3. The suprachiasmatic nucleus (SCN) immunofluorescent images indicate glial activation in a control (top row) and TBI induced (bottom row) mouse brain. CTB488 expression can be seen in green (column 2), GFAP in magenta (column 3), and IBA1 in yellow (column 4). An overlapped image of all three protein expression images can be seen in column 1.

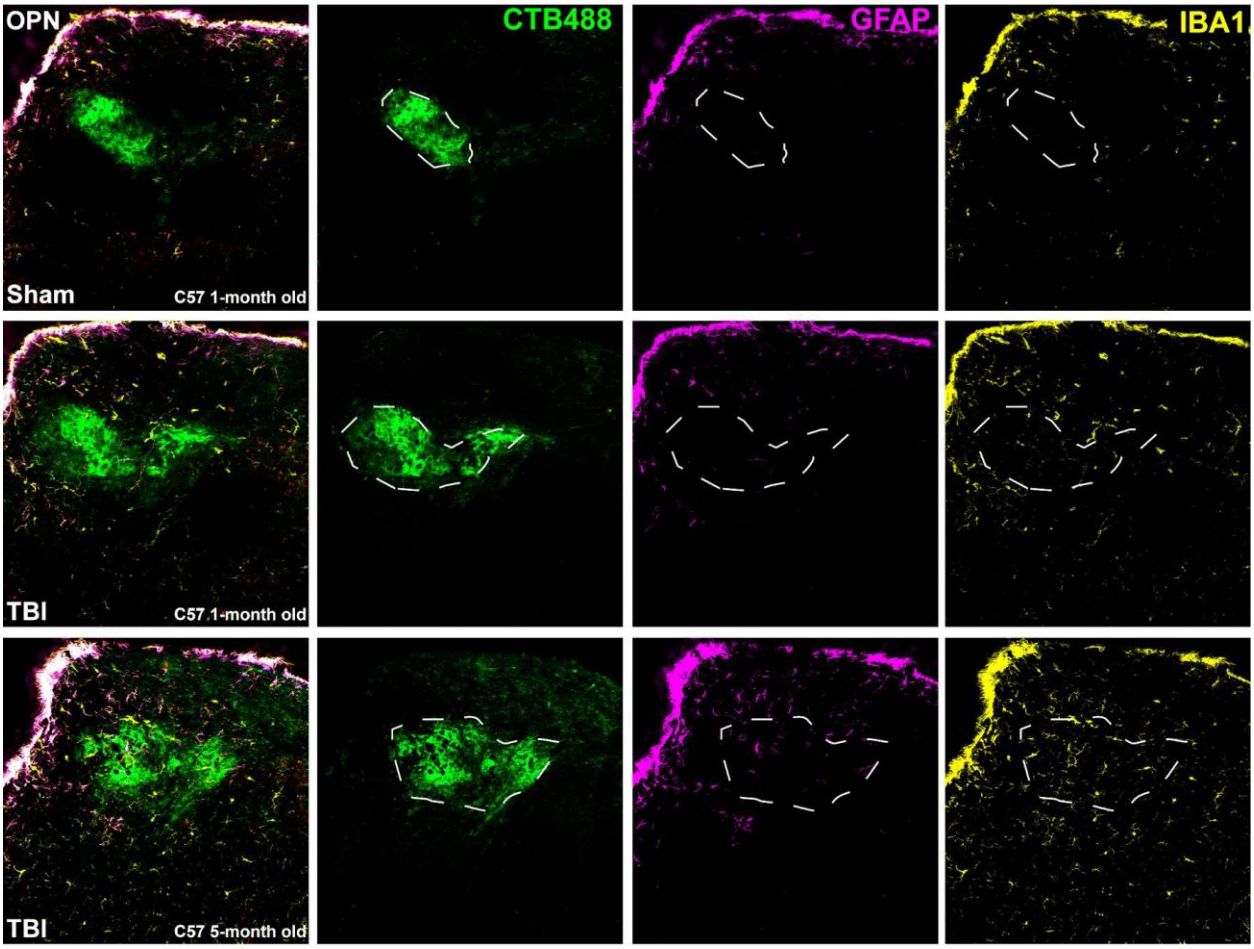

Figure 4. The olivary pretectal nucleus (OPN) immunofluorescent images indicate a lack of glial activation in a 1 month control (top row) and a 1 month and 5 month TBI induced (middle and bottom row respectively) mouse brain. CTB488 expression can be seen in green (column 2), GFAP in magenta (column 3), and IBA1 in yellow (column 4). An overlapped image of all three protein expression images can be seen in column 1.

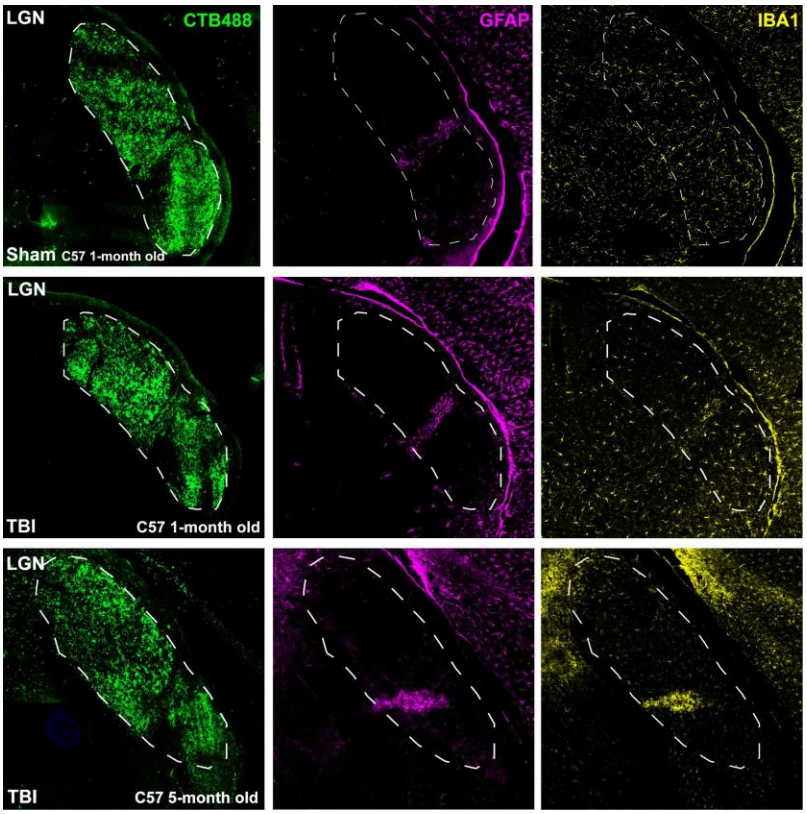

Figure 5. The lateral geniculate (LGN) immunofluorescent images indicate no glial activation in a 1 month control (top row) and some activation in a 1 month and 5 month TBI induced (middle and bottom row respectively) mouse brain. CTB488 expression can be seen in green (column 1), GFAP in magenta (column 2), and IBA1 in yellow (column 3).

4. Discussion

In this study we began by assessing the change in cellular morphology of M1 ipRGCs after TBI by staining the retina with melanopsin. Melanopsin stained ipRGCs were imaged in both TBI influenced and control mice. The three morphological metrics quantified from these images were somal area, dendritic branch points, and cell density. Together, these quantitative results can illustrate a holistic depiction of how ipRGC morphology changes across the cell. Interpreting the results of these three metrics together is important as different aspects of the cell can be differentially influenced by the TBI condition. These three metrics are a common way to account for the entire cell for morphological changes in ipRGCs (Lee & Schmidt, 2018). Results indicated a decrease in the number of branch points in the TBI induced 1-month old mice compared to controls. This suggests ipRGC morphological change after TBI in the younger age group. There was not a significant difference between the TBI and controls in the 5-month old

groups. This specific age variation in the branch point metric could be a result of ipRGC injury resistance that has been described in previous studies (Cui et al., 2015, Berry et al., 2019). Specifically, dendritic complexity measured by branch point counts has been indicated to remain static following proximal injury in previous studies using mice of a similar age (Tran et al., 2019). Since there was a significant decrease of dendritic complexity in our younger TBI mice but not the older, it seems that there may be an age-related correlation between changes in this type of morphology. Though this could easily be a result of having too few subjects, this trend could be particularly troubling as the major age group suffering from TBIs are the pediatric population which the 1 month old mice represent. It has been noted in optic nerve crush studies of mice 6-20 weeks of age, representing an adult neurological system, that ipRGCs are able to maintain dendritic complexity after injury. This was indicated by a lack of significant variation in dendritic area or arborization complexity (Tran et al., 2019). Though an optic nerve crush injury is a more proximal pathology than the TBI, it is relevant that this preliminary data aligns with documented adult ipRGC morphological trends. There is also literature suggesting a continuity of ipRGC function from pediatric through adult populations which seems to be countered by the data collected in this study (Adhikari et al, 2015).

The results from the somal size analysis indicated that both 1-month and 5-month groups saw a significantly decreased somal size in TBI induced mice compared to controls. It was also discovered that the 5-month old TBI somas were significantly smaller than the 1-month TBI somas. These results are interesting as they suggest a morphological change at all ages after suffering a TBI. A lack of age-related results presents as an inconsistency with the previous morphological metric which suggested the opposite. Some studies confer these results by indicating ipRGC cell soma size changes in relation to nerve injury by quickly swelling followed by apoptotic degradation of somal area (Ingham et al., 2009, Brännström et al., 1992). Changes in soma size indicate functional changes due to cellular form following function. Though functional differences were not described in this study, there is literature indicating this ipRGC functional change after TBI to complement this interpretation (Hartwick, 2015).

The final ipRGC morphological metric derived from this study was ipRGC cell density. This quantitative data provides evidence for the amount of neuron degeneration in the retina. Compared to controls, only the 5-month old TBI induced retina showed a significant decrease in cell density. This indicates an age-related effect where older ipRGCs are preferentially affected.

Many studies have already analyzed how ipRGC density is affected after injury. In nerve crush studies it has been noted that RGC degeneration occurs in mice as young as 1-3 months old (Daniel et al., 2018). Other injury types such as retinal damage by intraocular pressure elevation showed decreasing protective effects as mice reached 11 months of age (Cui et al., 2015). This is interesting as it suggests injury resistance variation across age. More distal injury, such as a V_1 cortical lesion, promotes inflammation and is associated with the atrophy of several other neural structures like the thalamus (Vigeveno et al., 2012). These findings align with the hypothesized link between TBI pathology resulting in the V1 region and promoting morphological changes in distant brain regions.

IpRGCs have diverged from other ganglion cell trends in many studies by exhibiting significantly higher survival percentages after proximal injury like an optic nerve crush (Vasalauskaite et al., 2019, Cui et al., 2015). Though there are studies citing M1 ipRGCs are not injury resistant in a neurodegenerative context (Lin et al., 2019), it is interesting that there is evidence that ipRGCs are exhibiting significant degeneration in this study. This could indicate TBI creates an environment where neuroprotective effects typically seen in ipRGCs are not effective. Potentially, inflammatory signaling is playing a role in deleteriously influencing older mice ipRGCs, similar to the effects of intraocular pressure (IOP) build up during glaucoma in the adult eye (Zavalía et al., 2011). Another potential facet of these results is the noted downregulation of melanopsin production after injury (Nadal-Nicolás et al., 2015). This was noted in mice after optic nerve injury but could indicate that the TBI context is causing a downregulation of melanopsin and cells are not being identified because of the experimental method rather than apoptosis. Further studies controlling for this effect would increase the confidence of the ipRGC cell density results.

Overall, the morphological metrics put together can start to describe a holistic effect the TBI has on ipRGCs. In each of the morphological metrics, there was at least one significant difference in TBI retina compared to controls. This supports the hypothesis that there will be morphological variations in ipRGCs after TBI. These results provide promising evidence for this case and encourages pursuing this hypothesis to solidify results with more data. The age-related effects however have variability in these cases that suggest a lack of consistent age-related morphological differences. Because the branch point indicated a significant morphological difference in 1-month ipRGCs only while cell density saw a significant difference in the 5-month

ipRGCs only, there is evidence for a complex age related variation in morphology. There are other mechanisms in which morphology of ipRGCs change independent of injury. It has been noted that process like late aging causes morphological variations in dendritic complexity of ipRGCs along with general ipRGC neuronal loss in degenerative diseases like Alzheimer's disease (Esquiva et al., 2017, Morgia et al., 2015, Lucas et al, 2003). There are also immunotoxins that can influence ipRGC morphology stimulated by mechanisms other than TBI (Ingham et al., 2009). These ipRGC influences should be controlled to prevent confounding morphological data.

To draw a more concrete link between the pathology of the brain to ipRGCs, brain tissue was analyzed in areas that link ipRGCs and the impacted cortical region. The biomarker analysis is likely indicating astrocyte hypertrophy and a microglial proliferation due to the common responses of these glia after this cortical injury type (Amat et al., 1996). This diverges from degenerative disease processes where both microglia and astrocytes can be seen to proliferate (McLean et al., 2005). The SCN images indicated an increase in gliosis biomarkers in the TBI induced mouse implying TBI was involved in creating a pathology at V1 which spread to the SCN. The same result is shown by the intergeniculate leaflet of the LGN. Both of these nuclei show how inflammatory pathology is traveling the pathway from V_1 injury site to ipRGCs. The OPN surprisingly did not show gliosis signaling despite also being a nucleus with a high ipRGC projection percentages in mice and primates (Hannibal et al., 2015, Morin & Studholme, 2015). There could be a variety of reasons for this result, potentially sharing less output neurons with the specific V1 region that got the CCI compared to other nuclei. A longer timeframe may also be needed to notice the neuroinflammation in subcortical areas like the OPN. Neuroinflammatory responses can be maintained in neural parenchyma up to 6 months after initial pathology (Caplan et al., 2015, Kumar et al., 2015). Overall, the results from the stained nuclei illustrate a somewhat consistent connection of pathology from the area of CCI to ipRGCs by way of specific intermediary sites in the brain.

The results from this experiment provide a proof of concept for further work on morphological analysis of ipRGCs after traumatic brain injury. A small sample size presented in this study is enough to decide the value of pursuing this work, but not enough to confidently support or refute the hypothesis. Adding more mice to control and experimental groups could strengthen the argument one way or another and is a task the lab plans to entertain in the future.

Additionally, the brain segment studies all appeared in qualitative form for this analysis. The creation of heat maps and illuminance to background metrics will aid in the qualitative evaluation of the pathological tract from injury to ipRGCs. Additional studies on the ipRGC physiological function after TBI could complete the form and function connection. Using a patterned electroradiograph (PERG) experiment could be used to indicate ganglion cell functioning and would be useful in generating complementary physiological data (Holder, 2001). A blue red pupillometer recording could also be used to generate this type of data (Hartwick, 2015).

5. Conclusion

The results from this preliminary data analysis indicate that there is a morphological impact on ipRGCs after traumatic brain injury. Due to the low sample size of the study, this trend is useful for indicating further experimentation rather than creating a confident statement for or against the hypothesis. Specific age-related effects seem to be a complicated facet of the ipRGC morphological response and may require the utilization of various different studies to provide an accurate depiction.

6. References

Adhikari, P., Pearson, C. A., Anderson, A. M., Zele, A. J., & Feigl, B. (2015). Effect of Age and Refractive Error on the Melanopsin Mediated Post-Illumination Pupil Response (PIPR). *Scientific reports, 5*, 17610. https://doi.org/10.1038/srep17610

Amat, J.A., Ishiguro, H., Nakamura, K., & Norton, W.T. (1996) Phenotypic diversity and kinetics of proliferating microglia and astrocytes following cortical stab wounds. *Glia, 16*(4). https://doi.org/10.1002/(SICI)1098-1136(199604)16:4<368::AID-GLIA9>3.0.CO;2-W

Bales, J.W. & Kim, L.J. (2019) Traumatic Brain Injury Overview and Practice Parameters. *Fundamentals of Neurosurgery*. https://doi.org/10.1007/978-3-030-17649-5_5

Barshikar, S., Bell, K.R. (2017) Sleep Disturbance After TBI. *Current Neurology and Neuroscience Reports, 17*(87). https://doi.org/10.1007/s11910-017-0792-4

Berry, M., Ahmed, Z., & Logan, A. (2019) Return of function after CNS axon regeneration: Lessons from injury-responsive intrinsically photosensitive and alpha retinal ganglion cells. *Progress in Retinal Eye Research, 71*, 57-67. https://doi.org/10.1016/j.preteyeres.2018.11.006

Brännström, T., Havton, L., & Kellerth, J. (1992) Restorative effects of reinnervation on the size and dendritic arborization patterns of axotomized cat spinal α-motoneurons

Caplan, B., Bogner, J., Brenner, L., Kumar, R.G., Boles, J.A., & Wagner, A.K. (2015) Chronic Inflammation After Severe Traumatic Brain Injury: Characterization and Associations With Outcome at 6 and 12 Months Postinjury. *Journal of Head Trauma Rehabilitation, 30*(6), 360-381. https://doi.org/10.1097/HTR.0000000000000067

Centers for Disease Control and Prevention (March 4, 2019) Traumatic Brain Injury & Concussion. https://www.cdc.gov/traumaticbraininjury/index.html

Ciuffreda, K.J., Kapoor, N., Rutner D., Suchoff, I.B., Han, M.E., & Craig, S. (2007) Occurrence of oculomotor dysfunctions in acquired brain injury: a retrospective analysis. *Optometry, 78*(4):155–161. doi:10.1016/j.optm.2006.11.011

Coxe, K., Hamilton, K., Harvey, H.H., Xiang, J., Ramirez, M.R., & Yang, J. (2018) Consistency and Variation in School-Level Youth Sports Traumatic Brain Injury Policy Content. *Journal of Adolescent Health, 62(*3), 255-264.

Cui, Q., Ren, C., Sollars, P.J., Pickard, G.E., & So, K.F. (2015) The injury resistant ability of melanopsin-expressing intrinsically photosensitive retinal ganglion cells. *Neuroscience*, 284:845–853. https://doi.org/10.1016/j.neuroscience.2014.11.002

Daniel, S., Clark, A. & McDowell, C. (2018) Subtype-specific response of retinal ganglion cells to optic nerve crush. *Cell Death Discovery. 4*, 67 https://doi.org/10.1038/s41420-018-0069-y

Dengler-Crish, C. M., Smith, M. A., Inman, D. M., Wilson, G. N., Young, J. W., & Crish, S. D. (2014). Anterograde transport blockade precedes deficits in retrograde transport in the visual projection of the DBA/2J mouse model of glaucoma. *Frontiers in neuroscience*, 8, 290. https://doi.org/10.3389/fnins.2014.00290

Dickson, D.W. & Weller, R.O. (2011) *Neurodegeneration: The Molecular Pathology of Dementia and Movement Disorders*. The International Society of Neuropathology.

Esquiva, G., Lax. P., Pérez-Santonja, J.J., García-Fernández, J.M., & Cuenca, N. (2017) Loss of Melanopsin-Expressing Ganglion Cell Subtypes and Dendritic Degeneration in the Aging Human Retina. *Frontiers in Aging Neuroscience.* https://doi.org/10.3389/fnagi.2017.00079

Georg, B.K., Bonhoeffer, T., & Hubener, M. (2012) Sensorimotor Mismatch Signals in Primary Visual Cortex of the Behaving Mouse. *Cellpress 74*(5), 809-815. https://doi.org/10.1016/j.neuron.2012.03.040

Hainline, B. & Stern, R.A. (2018) *Handbook of Clinical Neurology*. Elsevier.

Hannibal, J., Kankipati, L., Strang, C. E., Peterson, B. B., Dacey, D., & Gamlin, P. D. (2014). Central projections of intrinsically photosensitive retinal ganglion cells in the macaque monkey. The Journal of comparative neurology, 522(10), 2231–2248. https://doi.org/10.1002/cne.23588

Hattar, S., Liao, H. W., Takao, M., Berson, D. M., & Yau, K. W. (2002). Melanopsin-containing retinal ganglion cells: architecture, projections, and intrinsic photosensitivity. *Science*, *295*(5557), 1065–1070. https://doi.org/10.1126/science.1069609

Hayne, D.P. & Martin, P.R. (2019) Relating Photophobia, Visual Aura, and Visual Triggers of Headache and Migraine. *American Headache Society*. https://doi.org/10.1111/head.13486

Holder, G.E. (2001) Pattern electroretinography (PERG) and an integrated approach to visual pathway diagnosis. Prog Retin Eye Res. 20(4):531–561. https://doi.org/10.1016/s1350-9462(00)00030-6

Hubel, D.H. & Wiesel T.N. (1972) Laminar and columnar distribution of geniculo-cortical fibers in the macaque monkey. Journal of Comparative Neurology, 146(4). https://doi.org/10.1002/cne.901460402

Ingham, E.S., Günhan, E., Fuller, P.M., & Fuller, C.A. (2009) Immunotoxin-induced ablation of melanopsin retinal ganglion cells in a non-murine mammalian model. *The Journal of Comparative Neurology*. https://doi.org/10.1002/cne.22103

Jeon, S. W., & Kim, Y. K. (2016). Neuroinflammation and cytokine abnormality in major depression: Cause or consequence in that illness?. World journal of psychiatry, 6(3), 283–293. https://doi.org/10.5498/wjp.v6.i3.283

Jones, A., & Jarvis, P. (2017). Review of the potential use of blood neuro-biomarkers in the diagnosis of mild traumatic brain injury. *Clinical and experimental emergency medicine*, *4*(3), 121–127. https://doi.org/10.15441/ceem.17.226

Kumar, R., Boles, J., & Wagner, A. (2015) Chronic Inflammation After Severe Traumatic Brain Injury: Characterization and Associations With Outcome at 6 and 12 Months Postinjury. *Journal of Head Trauma Rehabilitation. 30*(6), 369–381. https://doi.org/10.1097/HTR.0000000000000067

Kyle, W., David, P., & John, C. (2019) Reconsidering Hypothermia for Severe Traumatic Brain Injury, *Neurosurgery, 85(*2), E184, https://doi.org/10.1093/neuros/nyz036

Lee, S.K. & Schmidt, T.M. (2018) Morphological Identification of Melanopsin-Expressing Retinal Ganglion Cell Subtypes in Mice. *Mouse Retinal Phenotyping, 1753*. https://doi.org/10.1007/978-1-4939-7720-8_19

Li, Z., Ji, X., Zheng, T., Zhang, Y., & Li, Z. (2109) Effect of long-term and short-term mild hypothermia in severe traumatic brain injury: a comparative study. *Europe PMC, 31*(12):1440-1444. https://doi.org/10.3760/cma.j.issn.2095-4352.2019.12.002

Lin, M., Liao, P., Chen, H., Chang, C., Chen, S., & Chern, Y. (2019) Degeneration of ipRGCs in Mouse Models of Huntington's Disease Disrupts Non-Image-Forming Behaviors Before Motor Impairment. Journal of Neuroscience, 29(8), 1505-1524. https://doi.org/10.1523/JNEUROSCI.0571-18.2018

Lu, J., Marmarou, A., Lapane, K. L., & IMPACT Investigators (2012). Impact of GOS misclassification on ordinal outcome analysis of traumatic brain injury clinical trials. *Journal of neurotrauma, 29*(5), 719–726. https://doi.org/10.1089/neu.2010.1746

Lucas, R.J., Hattar, S., Takao, M., Berson, D.M., Foster, R.G., & Yau, K.W. (2003) Diminished Pupillary Light Reflex at High Irradiances in Melanopsin-Knockout Mice. *Science, 299*(5604), 245-247. https://doi.org/10.1126/science.1077293

McLean, J.R., Sanelli, T.R., Leystra-Lantz, C., He, B.P., and Strong, M.J. (2005) Temporal profiles of neuronal degeneration, glial proliferation, and cell death in hNFL(+/+) and NFL(−/−)mice. *Glia*. https://doi.org/10.1002/glia.20218

Morgia, C., Ross-Cisneros, F.N., Koronyo, Y., Hannibal, J., Gallassi, R., Cantalupo, G., Sambati, L., Pan, B.X., Tozer, K.R., Barboni, P., Provini, F., Avanzini, P., Carbonelli, M., Pelosi, A., Chui, H., Liguori, R., Baruzzi, A., Koronyo-Hamaoui, M., Sadun, A.A, & Carelli, V. (2015) Melanopsin retinal ganglion cell loss in Alzheimer disease. *Annals of Neurology, 79*(1). https://doi.org/10.1002/ana.24548

Morin, L. P., & Studholme, K. M. (2014). Retinofugal projections in the mouse. The Journal of comparative neurology, 522(16), 3733–3753. https://doi.org/10.1002/cne.23635

Nadal-Nicolás, F.M., Madeira, M.H., Salinas-Navarro, M., Jiménez-López, M., Galindo-Romero, C., Ortín-Martínez, A., Santiago, A.R., Vidal-Sanz, M., & Agudo-Barriuso, M. (2015) Transient Downregulation of Melanopsin Expression After Retrograde Tracing or Optic Nerve Injury in Adult Rats. *Investigative Ophthalmology & Visual Science 56*, 4309-4323. https://doi.org/10.1167/iovs.15-16963

Rogers, Sandra (2018) Classification of Traumatic Brain Injury Severity Complexities in Retrospective Data, *Sigma Theta Tau International's 29th International Nursing Research Congress*

Saatman, K.E., Duhaime, A., Bullock, R., Maas, A.I.R., Valadka, A., & Manley., G.T. (2010) Classification of Traumatic Brain Injury for Targeted Therapies. *Journal of Neurotrauma*, *25*(7), 719-738. http://doi.org/10.1089/neu.2008.0586

Sargeant, M., Sykes, E., Saviour, M., Sawhney, A., Calzolari, E., Arthur, J., McGoldrick, A., & Seemungal, B.M. (2018) The utility of the Sports Concussion Assessment Tool in hospitalized traumatic brain injury patients, *Journal of Concussion*, (2), 1-10.

Teasdale G, Jennett B. (1976) Assessment and prognosis of coma after head injury. *Acta Neurochir 34*(1-4):45–55. doi:10.1007/bf01405862

Thomas Jefferson University (2019) Disease Staging. https://www.jefferson.edu/university/skmc/research/research-medical-education/Disease_Staging.html

Tran, N.M., Shekhar, K., Whitney, I.E., Jacobi, A., Benhar, I., Hong, G., Yan, W., Adiconis, X., Arnold, M.E., Lee, J.M., Levin, J.Z., Lin, D., Wang, C., Lieber, C.M., Regev, A., He, Z., & Sanes J.R. (2019) Single-cell profiles of retinal neurons differing in resilience to injury reveal neuroprotective genes. *BioRxiv* 711762. https://doi.org/10.1101/711762

Vasalauskaite, A., Morgan, J.E., & Sengpiel, F. (2019) Plasticity in Adult Mouse Visual Cortex Following Optic Nerve Injury. *Cerebral Cortex, 29*(4), 1767–1777. https://doi.org/10.1093/cercor/bhy347

Vigeveno, R.M., Wiebenga, O.T., Wattjes, M.P., Geurts, J.J.G., & Barkhof, F. (2012) Shifting imaging targets in multiple sclerosis: From inflammation to neurodegeneration. *Journal of Magnetic Resonance Imaging, 36*(1). https://doi.org/10.1002/jmri.23578

Winblad, B., Ankarcrona, M., Johansson, G., Novak, P., Peter-Thelin, E., Zetterberg, H., & Blennow, K. (2019) Head trauma in sports and risk for dementia, *Journal of Internal Medicine, 285(6)***285**, 591-593.

Zavalía, N., Plano, S.A., Fernandez, D.C., Lanzani, M.F., Salido, E., Belforte, N., Sarmiento, M.I.K., Golombek, D.A., & Rosenstein, R.E. (2011) Effect of experimental glaucoma on the non-image forming visual system. *Journal of Neurochemistry, 117*(5). https://doi.org/10.1111/j.1471-4159.2011.07260.x